Condensation and Laser Attenuation in Water Plumes from a Laser-Propelled Rocket

Guy M. Weyl* and Ven H. Shui†
Avco Everett Research Laboratory, Inc., Everett, Mass.

This paper investigates condensation and absorption of CO_2 laser radiation in water-vapor plumes at various altitudes with specific application to laser propulsion of rockets. At high altitudes ($\geq$90 km) the plume was modeled as an expansion into vacuum; the expansion leads to cooling and condensation. Absorption both by condensed water droplets and by water vapor was found to be negligible ($\simeq 5\times10^{-3}$). At intermediate and low altitudes ($\leq$20 km) the plume cools by entraining ambient air. We find that for typical engine conditions condensation is unlikely if the ambient air is dry. Absorption by water vapor was found to be negligible at 20 km ($\leq 10^{-3}$) and small at sea level ($\approx$4%). However, limited broadband water-vapor absorption data indicate that the actual absorption could be up to a hundred times greater due to high-temperature absorption lines not included in the present calculations. High-resolution transmissivity measurements at the exact location of the CO_2 lines are needed for definite conclusions to be drawn near sea level.

Nomenclature

A_b = absorption, Eq. (17)
A = area
B = constant, Eq. (5)
C_p = specific heat at constant pressure
D = diameter
f = laser pulse rate
g = acceleration of gravity
ΔH = enthalpy of formation
h = enthalpy per unit mass
I = specific impulse
J = condensation rate, Eq. (12)
k = Boltzmann constant
L = distance, Eq. (18)
m = vehicle mass
$\dot{m}$ = mass flow rate
M = Mach number
p = partial pressure of water vapor
P = total pressure
Q_a, Q_s = Mie absorption, scattering efficiencies
Q_R, Q_V = rotational, vibrational partition functions
r = radial distance
r^* = critical radius, Eq. (13)
R = radius
$\mathfrak{R}$ = gas constant, Eq. (1)
s = surface tension
$S(T)$ = line intensity
t = time
T = temperature
u = velocity
w = integrated water mass per unit area
x = axial distance
Z = compressibility factor
α = absorption coefficient
β = acceleration in units of g
γ = ratio of specific heats
Γ = proportionality constant, Eq. (12)
ϵ = energy of lower vibrational state
θ = polar angle
θ_v = vibrational spacing in units of temperature
θ_∞ = Prandtl-Meyer expansion angle
η = energy efficiency of engine
λ = wavelength
μ = molecular mass
ν = wave number
ν_0 = wave number at line center
$\Delta\nu$ = line width
ρ = mass concentration of water vapor
ρ_w = density of condensed water
σ = cross section
τ = expansion time
ψ_x = mole fraction of specie x

Subscripts

a = ambient value
c = at condensation point
e = exit condition
M = refers to mach disk
p = refers to plume
s = stagnation condition
0 = reference value

Received May 18, 1977; presented as Paper 77-696 at the AIAA 10th Fluid and Plasmadynamics Conference, Albuquerque, N. Mex., June 27-29, 1977; revision received Sept. 6, 1977.

Index categories: Jets, Wakes, and Viscid-Inviscid Flow Interactions; Thermophysical Properties of Matter; Lasers.

*Principal Research Scientist.

†Principal Research Scientist. Member AIAA.

I. Introduction

In the laser-propelled rocket concept,[1-4] laser energy from a distant source would be absorbed by the fuel inside the rocket chamber, thereby providing high pressures and temperatures. Absorption mechanisms could be either molecular absorption by the fuel at lower temperatures ($3000 < T < 5000$ K), or electron-neutral and electron-ion inverse bremsstrahlung absorption at higher temperatures ($T > 6000$ K). We show in Fig. 1 two engine configurations corresponding to CW and pulsed operation. In Fig. 1a the laser beam is focused by a reflecting nozzle into a small focal volume inside the chamber, maintaining a laser supported combustion wave,[5] which is stationary with respect to the chamber and subsonic with respect to the gas flow. In Fig. 1b a collimated laser beam ignites a laser supported detonation (LSD) wave[6] at the rear end of a layer of gaseous propellant; the wave travels supersonically toward the laser beam. The laser beam would be turned off after the whole layer has been processed, and would be turned on again after the gas (plasma) has expanded out of the nozzle and a new layer of gas has been introduced into the chamber.‡

‡This engine configuration was first suggested by D. Reilly. Experiments in which LSD waves are generated in N_2 and He gases under the geometry shown in Fig. 1b are presently being conducted at Avco.

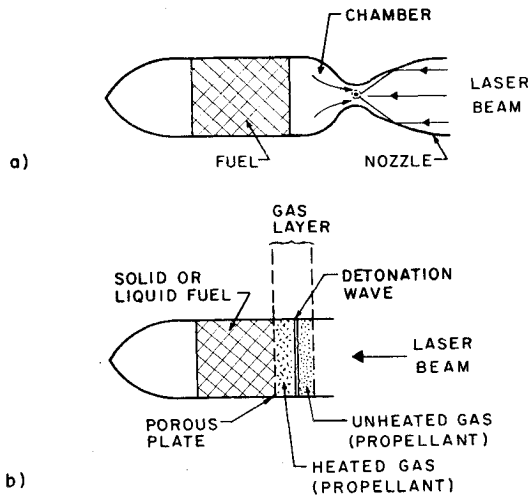

Fig. 1 Configuration for laser propelled rocket: a) CV operation with formation of subsonic laser supported combustion wave; b) pulsed operation with formation of laser supported detonation wave.

Large specific impulses ($I > 800$ sec) seem obtainable in view of the high temperatures at which laser-supported absorption waves operate and this consideration combined with the fact that the source of laser power could be ground based, makes the laser-propelled rocket concept an attractive one.

Water (or ice) appears to be an ideal fuel for laser-propelled vehicles because 1) it is cheap, 2) it does not pollute, and 3) it has a low molecular mass in the vapor phase and high density under ambient conditions (as opposed to N_2, H_2, He, etc., which have to be stored under cryogenic conditions).

A possible drawback to the use of water as opposed to liquid N_2, for example, is the condensation that may occur in the plume and the deleterious effect that condensation may have on laser propagation from the transmitter to the laser-powered thruster. Also, high-temperature H_2O is an absorber of 10.6 μm radiation. In this work we study the effect of water-vapor transmission and water condensation on laser propagation in three regimes: 1) high-altitude plume which expands into vacuum, 2) plume at 20-km altitude, and 3) low-altitude plume near sea level. In Sec. II we summarize the data on absorption by water vapor at 10.6 μm wavelength. In Sec. III we calculate the exit conditions at the rocket nozzle for a typical vehicle with mass 8000 kg, acceleration βg ($\beta \approx 3$), and specific impulse 800 sec. High-altitude plume condensation is calculated in Sec. IV, and low and intermediate altitude plumes are treated in Sec. V. Absorption of the laser beam in these plumes is also considered in these sections. Our conclusions will be presented in Sec. VI.

II. Absorption by Water Vapor and Water Droplets

There is a great deal of information on absorption by water vapor at 10.6 μm at room temperature. A recent review of the data was made by Adiks et al.,[7] and the present belief is that absorption is due to a water-vapor dimer, the absorption coefficient being given by

$$\alpha = 1.76\times 10^{-3}\rho + 0.42\times 10^{-6}\rho^2 \exp(-\Delta H/\Re T)\,\mathrm{km}^{-1} \quad (1)$$

where $\Delta H = -4500$ cal/mole is the binding energy of the dimer and ρ, the water-vapor concentration in g/m^3.

There is much less information on absorption by water vapor at high temperatures. Experimental measurements of water-vapor absorption at temperatures $T \simeq 2000$°C and $P \simeq 1$ atm have been reported by Ludwig et al.[8] and are several orders of magnitude larger than those given by Eq. (1). At high temperatures, vibration-rotation lines due to high-lying levels appear in the 10-μm window and are the main cause for absorption. Unfortunately, the measurements of Ref. 8 were taken with a resolution of 25 cm^{-1}, and the absorption coefficient at the location of the CO_2 laser lines is unknown. We have used the compilation of spectral information on H_2O made by McClatchey[9] to estimate the absorption coefficient at the specific wavelengths of the CO_2 laser. The McClatchey tape[9] contains information on H_2O lines that appear at room temperature only, and represents a lower bound on H_2O absorption, since other lines may become important at higher temperatures. The line shape due to collision broadening is given by

$$\alpha(\nu) = \frac{S(T)\Delta\nu}{\pi[(\nu-\nu_0)^2+\Delta\nu^2]} \quad (2)$$

The line width $\Delta\nu$ is proportional to pressure and varies inversely with the square root of temperature. The variation of line intensity per atom with temperature is given by

$$S(T) = \frac{S_0}{Q_V Q_R}\exp\left(-\frac{\epsilon}{kT}\right) \quad (3)$$

For water vapor at temperatures below 3000 K, $Q_R \propto T^{3/2}$ and $Q_V \simeq [1-\exp(-\theta_v/T)]^{-1}$, where $\theta_v = 2290$ K (corresponding to the 6.3 μm band of H_2O). At standard temperature and pressure the line width of an H_2O line is estimated to be[10] 0.07 cm^{-1}, and we find that, for $P \lesssim 1$ atm, the CO_2 lines fall well into the wings of the H_2O lines compiled by McClatchey. The absorption coefficient α at T and P is obtained from the absorption coefficient α_0 at T_0 and P_0 by combining Eqs. (2) and (3). We obtain

$$\frac{\alpha}{\alpha_0} = \left(\frac{p}{p_0}\right)^2\left(\frac{T_0}{T}\right)^3 \exp\left[-\frac{\epsilon}{k}\left(\frac{1}{T}-\frac{1}{T_0}\right)\right] \times\left[\frac{1-\exp(-\theta_v/T)}{1-\exp(-\theta_v/T_0)}\right] \quad (4)$$

where one factor $(p/p_0)(T_0/T)$ takes into account the varying amount of absorber (assumed pure) in the path, another factor $(p/p_0)(T_0/T)^{1/2}$ takes into account the pressure broadening of the lines, and the remaining factors are due to the partition functions. Absorption of the $P(16)$–$P(24)$ lines of CO_2 by the H_2O vapor was found to follow Eq.

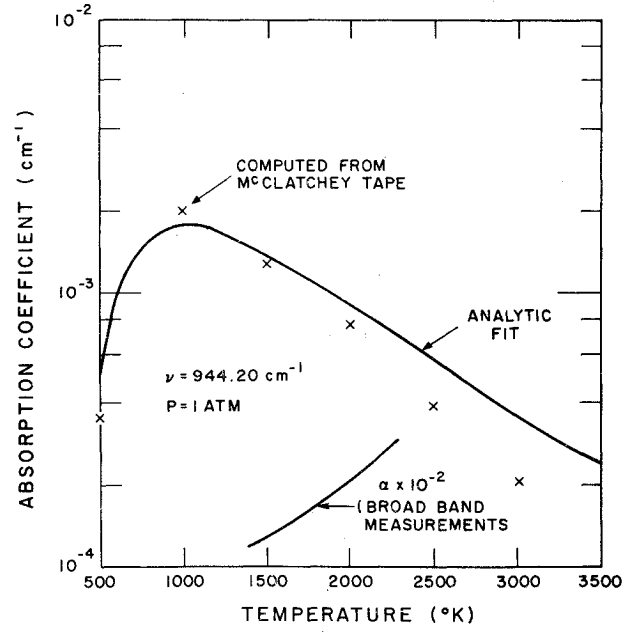

Fig. 2 Absorption coefficient for the $P(20)$ line of CO_2.

Table 1 Parameters entering in Eq. (5)

CO_2 line, ν_0 (cm)$^{-1}$	P(16) 947.74	P(18) 945.98	P(20) 944.20	P(22) 942.38	P(24) 940.55
B[cm^{-1} Atm^{-2}(K)^3]	1.53×10^6	4.48×10^6	5.55×10^7	4.1×10^6	5.5×10^6
ϵ/k (K)	1870	2950	3330	3150	3010

(4) fairly well in the range 300 to 2500 K and can be represented with an accuracy better than 30% by

$$\alpha = B\frac{p^2}{T^3}\exp\left(\frac{-\epsilon}{kT}\right)\left[1-\exp\left(\frac{-2290}{T}\right)\right]\text{cm}^{-1} \tag{5}$$

where p is in atmospheres and B and ϵ are given in Table 1. A comparison of the analytic fit with the results of the McClatchey tape is shown in Fig. 2, for the $P(20)$ line of CO_2.

For condensed water droplets, the attenuation of radiation can be represented by the attenuation cross section,

$$\sigma = \pi R^2 (Q_a + Q_s) \tag{6}$$

where the absorption and scattering efficiencies can be obtained from Mie theory. For particle radii $R<5\mu$m and $\lambda = 10.6\ \mu$m, we have $Q_a \gg Q_s$, and we can approximate Q_a by

$$Q_a = 1200\,R \tag{7}$$

where R is in cm.

III. Rocket Nozzle Exit Conditions

Consider a pulsed device which has a vapor expansion time much longer than the laser pulse time. The equation of motion, averaged over a large number of laser pulses, is

$$m\frac{dV}{dt} = \dot{m}u_e = (\rho_e u_e A_e)\tau_e f\, u_e \tag{8}$$

For constant vehicle acceleration, we write $dV/dt = \beta g$, and obtain

$$\rho_e = \beta m/(I^2 g\,\tau_e f\, A_e) \tag{9}$$

where $I = u_e/g$ is the specific impulse (typically ≈ 800 sec).

The exit enthalpy h_e and the stagnation enthalpy h_s are related by the equations

$$h_e/h_s = 1-\eta \tag{10}$$

$$h_s - h_e = u_e^2/2 = I^2 g^2/2 \tag{11}$$

The enthalpy of water vapor for the range of pressures varying from 10^{-3} to 10^{+2} atmospheres and temperatures from 300 K to 5700 K is shown in the form of a Mollier diagram in Fig. 3. This Mollier diagram was generated by using an equilibrium chemistry calculation[11] which incorporates the thermophysical properties contained in the JANAF tables.[12] Other calculations that can be found in the literature are not sufficient for our purpose because they do not extend either to high enough temperatures[13] or to low enough pressures.[14]

As a typical example we consider an engine appropriate for single stage launch from Earth to a transfer ellipse to geosynchronous orbit.[15] The mass of the vehicle is taken to be 8000 kg, $\beta = 3$, and the required specific impulse is in the 800-1000-sec range.[15] The stagnation conditions are (point A in Fig. 3) $p_s = 80$ atm, $T_s = 5700$ K, $h_s = 5.3\times10^4$ J/g. Exit conditions corresponding to isentropic expansion and an engine efficiency $\eta = 0.5$ can be obtained from Eqs. (10) and (11) and the Mollier chart for H_2O. We get point B in Fig. 3, where $p_e \simeq 0.06$ atm. At low altitudes where the ambient pressure P_a is greater than 0.06 atm, we shall allow the nozzle expansion to proceed only until $p_e = P_a$. Thus, at sea level, we have $p_e = P_a = 1$ atm, and the exit conditions are represented by point C. The exit parameters for the high-altitude plume (point B) and low-altitude plume (point C) are shown in Table 2. The corresponding exit areas A_e were obtained by use of Eq. (9).

Table 2 Plume conditions

M_e	A_e, cm^2	u_e, cm/sec	T_e, K	ρ_e, g/cm^3	P_e, atm	Z_e	I, sec
High-altitude plume							
4.45	1.5×10^4	7.6×10^5	3000	2.8×10^{-6}	0.06	1.6	860
Low-altitude plume							
3.17	1.78×10^3	6.48×10^5	3600	3.2×10^{-5}	1	1.9	650

IV. Absorption in High-Altitude Plumes

For the high-altitude case we assume that the plume expands into vacuum, that the chemistry is frozen, and that the ratio of specific heats of water vapors is $\gamma = 1.33$ (frozen vibration, 3 degrees of freedom for rotation in equilibrium). The structure of highly underexpanded jets has been investigated by many authors[16-18] and we shall summarize only results relevant to this research. The jet geometry is shown in Fig. 4. At distances sufficiently far away from the nozzle the flow is practically radial and the density varies as r^{-2}. Also, at a given radial position the density varies as $[\cos(\pi/2)(\theta/\theta_\infty)]^{2/(\gamma-1)}$. The results quoted earlier do not take into account the effect of condensation. However, since the enthalpy of condensation (3×10^3 J/g) is ten times less than the kinetic energy of the expanding plume (3×10^4 J/g) we expect that the effect of condensation on the flow will be small.

Inside the barrel shock the expansion can be taken as isentropic for continuum flow. The barrel shock terminates by a Mach disk in which the overexpanded jet is shocked into pressure equilibrium with the surrounding air. In our treatment of the high-altitude expansion we consider free expansion of the gas and are therefore considering gas properties upstream of the Mach disk. The location of the Mach disk has been calculated from entropy considerations by Young[19] who finds that this distance scales as

$$x_M = C(\gamma)\,(P_e/P_a)^{1/2} D$$

where $C(\gamma)$ is a weakly dependent function of γ. For $\gamma = 1.33$ we take $C(\gamma) = 0.7$. We calculate, as will be shown later, for the specific engine considered, that condensation occurs approximately 140-m behind the vehicle. Using $D = 1.4$ m, $P_e = 0.06$ atm, and setting $x_M > 140$ m, we find that our treatment of free expansion up to the condensation point is only valid for $P_a < 3\times10^{-6}$ atm, i.e., for altitudes above 90 km.

A. Condensation and Its Effect on Laser Propagation

The rate of formation of condensation nuclei of critical radius r^*, following condensation theory, is given by[20]

$$J = \frac{\Gamma}{\rho_w}\frac{\rho^2}{\mu^2}\left(\frac{2s\mu}{\pi}\right)^{1/2}\exp\left[-\frac{4\pi(r^*)^2 s}{3kT}\right]\text{nuclei cm}^{-3}\text{sec}^{-1} \tag{12}$$

where the surface tension s for ice is 96 dyn/cm and the critical radius of a condensation nucleus is related to the

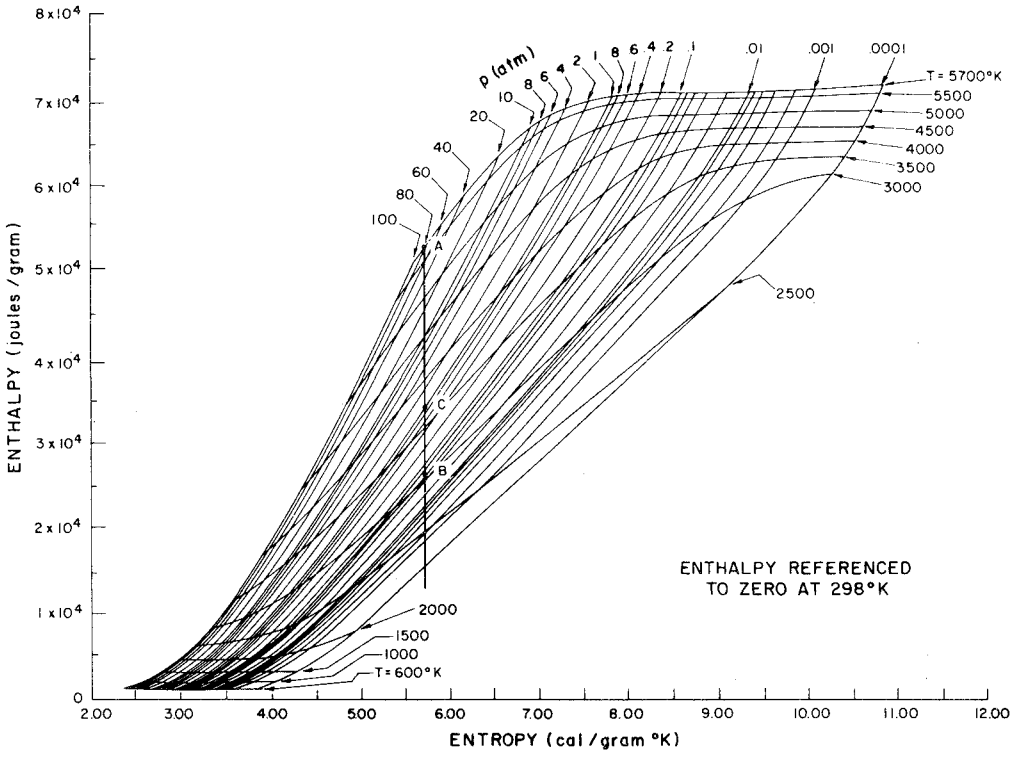

Fig. 3 Mollier diagram for water vapor.

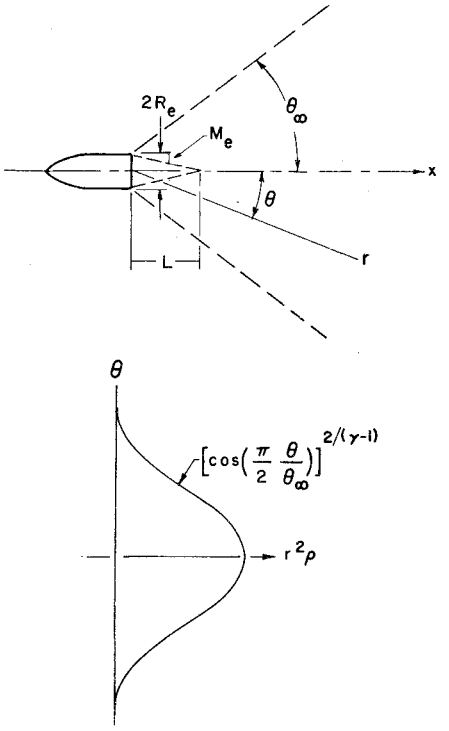

Fig. 4 Geometry for jet expansion into vacuum.

supersaturation ratio as follows

$$r^* = \frac{2s\mu}{\rho_w kT \ln(p/p_{sat})} \tag{13}$$

The factor Γ varies over several orders of magnitude depending on the nucleation theory considered.[20] Because of the strong temperature dependence of the exponent, however, the actual value of Γ turns out to be not too important. In our calculations we take $\Gamma = 1$ which should be a good approximation for water vapor. We obtain the condensation rate by multiplying Eq. (14) by the factor $4\pi/3(\rho_w/\mu)r^{*3}$ which is number of water molecules in a critical condensation nucleus. The saturated vapor pressure of ice is approximately given by

$$p_{sat} \approx 4 \times 10^7 \exp(-6170/T) \text{ atm} \tag{14}$$

By using Eqs. (12-14) and standard relationships for isentropic expansion[21] we can relate downstream temperature, supersaturation ratio, and condensation rate to the local Mach number. We can then calculate the normalized condensation rate which is the mass fraction of plume condensed in the characteristic time r/u. The flow properties are related to the radial position through the mass continuity equation

$$\rho_e u_e A_e = \rho u \pi r^2 \int_0^{\pi/2} \left[\cos\left(\frac{\pi}{2}\frac{\theta}{\theta_\infty}\right)\right]^{2/(\gamma-1)} \sin\theta d\theta \tag{15}$$

For exit conditions listed in Table 2 we find that $M_e = 4.45$, $\theta_\infty = 69$ deg. The results are plotted in Fig. 5. The temperature and supersaturation ratio are shown in Figs. 5a and 5b. The flow becomes saturated when $T = 200$ K. From Fig. 5c one sees that condensation occurs at $T = 150$ K, when the normalized condensation rate is of order unity. The conditions at the condensation front are $\rho_c = 3.5 \times 10^{-10}$ g/cm^3, $u_c \approx u_e = 7.6 \times 10^5$ cm/sec, $r \approx 140$ m, and the integrated water content per unit area along the axis is

$$w = \int_{r_c}^{\infty} \rho dr = \rho_c r_c = 5 \times 10^{-6} \text{g cm}^{-2} \tag{16}$$

The total absorption by water droplets along the axis can then be calculated from Eqs. (6, 7, and 16); the result is

$$A_b = 1 - \exp(-900w) \approx 5 \times 10^{-3} \tag{17}$$

That is, condensation has a negligible effect on laser propagation.

B. Absorption by Water Vapor

Consider, as before, the streamline along the axis of the vehicle which contains the largest amount of vapor. The

vapor starts expanding when the Mach line from the edge of the nozzle intersects the axis of the vehicle. This occurs at a distance.

$$L = R_e M_e \approx 300 \text{ cm} \tag{18}$$

We thus have $T = T_e$ and $\rho = \rho_e$ for $x < L$. For $x > L$ we approximate the flowfield by

$$\rho(x) = \rho_e L^2/[(x-L)^2 + L^2] \tag{19}$$

and use isentropic relations to calculate T and p. We can use Eq. (5) to calculate the water-vapor absorption.

$$A_b = 1 - \exp\left(-\int_0^{x_c} \alpha dx\right) \tag{20}$$

Frozen Vibration, Frozen Chemistry

Let the absorption coefficient, $\alpha = \alpha_e$ at the nozzle exit. Then at a location x the absorption coefficient is

$$\alpha(x) = \alpha_e \left[\frac{P(x)}{P_e}\right]^2 \left[\frac{T_e}{T(x)}\right]^3 = \alpha_e \left(\frac{\rho}{\rho_e}\right)^{3-\gamma} \tag{21}$$

By subsituting Eq. (21) into Eq. (20) and carrying out the integration, we obtain

$$\int_0^{x_c} \alpha dx = 1.64 \alpha_e L \tag{22}$$

Equilibrium Vibration, Frozen Chemistry

By using Eq. (4) and expressing p, ρ, and x as functions of $z = (\rho/\rho_e)$, we obtain

$$\int_0^{x_c} \alpha dx = \alpha_e L + \frac{\alpha_e L}{2[1-\exp(-\theta_v/T_e)]} \times \int_{\rho_e/\rho_e}^{1} dz \left(\frac{z}{1-z}\right)^{1/2} z^{1-\gamma} \exp\left[-\frac{\epsilon}{kT_e}(z^{1-\gamma}-1)\right] \times \left[1-\exp\left(\frac{-\theta_v}{T_e} z^{1-\gamma}\right)\right] \tag{23}$$

Numerical integration of the integral for $\rho_c \ll \rho_e$, $\gamma = 1.33$ and $T_e = 3000$ K yields

$$\int_0^{x_c} \alpha dx = \alpha_e L \left\{1 + \frac{0.71}{2[1-\exp(-\theta_v/T_e)]}\right\} = 1.66 \alpha_e L \tag{24}$$

This result is, for all practical purposes, the same as that for frozen vibration, Eq. (22).

The absorption coefficient for the $P(20)$ line of CO_2 can be calculated from Eq. (5). The result is

$$\alpha_e = 1.3 \times 10^{-6} \text{ cm}^{-1} \tag{25}$$

Thus $\alpha_e L = 4 \times 10^{-4}$, and absorption by water vapor is negligible.

V. Absorption and Condensation in Lower-Altitude Plumes

At low altitudes the external pressure prevents the jet of vapor from expanding freely and cooling of the jet arises from entrainment of and mixing with the ambient air. The cooling of the jet and possible condensation depends on 1) the amount of air entrained, 2) the ambient temperature, and 3) the degree of recombination of the partially dissociated water vapor.

We have used a three-dimensional axisymmetric computer code which numerically solves mass, momentum, enthalpy, and species conservation equations using turbulent diffusivity and finite rate chemistry. Calculations have been made at 20-km altitude ($P_a = 0.06$ atm) and at sea level ($P_a = 1$ atm) and will now be discussed.

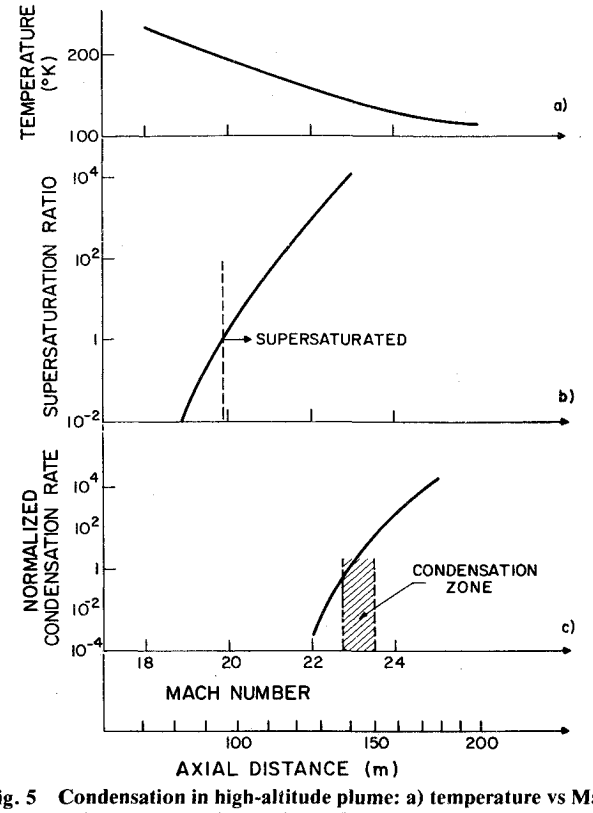

Fig. 5 Condensation in high-altitude plume: a) temperature vs Mach number, b) supersaturation ratio vs Mach number, c) normalized condensation rate vs Mach number.

A. Condensation of Water Vapor in Plumes

Before presenting results of our numerical calculations, we shall first discuss the possibility of condensation in the plume and show from general energy considerations that condensation is unlikely to occur if the ambient air temperature is larger than 230 K. Consider a mass m_p of plume material (pure vapor) that entrains a mass m_a of air. Assume that the exit pressure P_e is the same as the ambient pressure P_a. Conservation of momentum and energy yields

$$m_p u_e = (m_a + m_p) u \tag{26}$$

$$m_p(h_e + \tfrac{1}{2}u_e^2) + m_a h_a(T_a) = m_p h_p(T) + m_a h_a(T) + \tfrac{1}{2}(m_p + m_a) u^2 \tag{27}$$

We have assumed in the foregoing that the ambient air is at rest and that the vehicle velocity is much less than u_e. By eliminating u between Eqs. (26) and (27), and then neglecting small terms in the resulting expression, one can show that

$$p = \frac{\mu_a}{\mu_{H_2O}} \frac{C_{pa}(T - T_a)}{h_s} P_a \tag{28}$$

In deriving Eq. (28) we have assumed $p/P_a \ll 1$ and that recombination is complete.

A necessary condition for condensation to occur is

$$p \geq p_{sat} \tag{29}$$

By combining Eqs. (14) and (28), this condition becomes

$$\frac{\mu_a}{\mu_{H_2O}} \frac{C_{pa}}{h_s} P_a \geq \frac{4 \times 10^7 \exp(-6170/T)}{(T - T_a)} \tag{30}$$

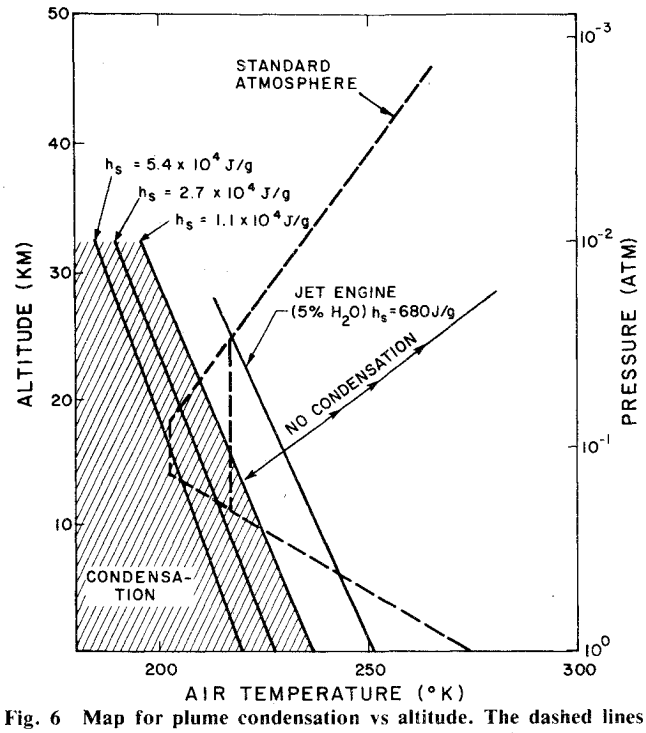

Fig. 6 Map for plume condensation vs altitude. The dashed lines correspond to the temperature profiles for 30 deg and 60 deg Northern latitude standard atmospheres in July.

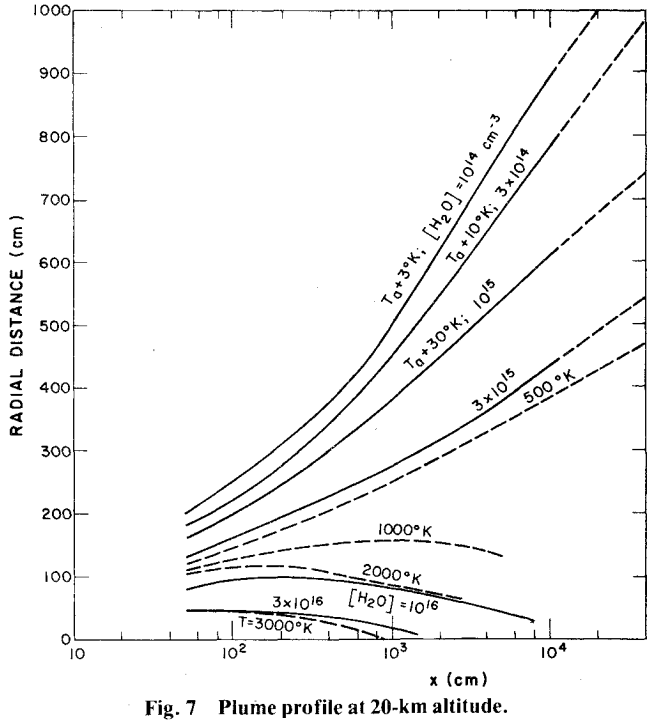

Fig. 7 Plume profile at 20-km altitude.

The right-hand side of Eq. (30) has a local minimum at $T/T_a = 1.013$, and for solutions of practical interest this minimum defines the minimum pressure P_a vs T_a for which condensation can occur, or alternatively, for any given P_a, the maximum T_a above which condensation *cannot* occur. For example, for $h_s = 5.3\times10^4$ J/g and $P_a = 1$ atm, T_a must be less than about 220 K in order to have condensation. Such condensation boundaries are plotted on the altitude-ambient temperature map in Fig. 6 for several values of h_s. The ambient temperature for a standard atmosphere is also plotted in Fig. 6. We note that condensation is unlikely to occur and may be possible only in a small altitude range

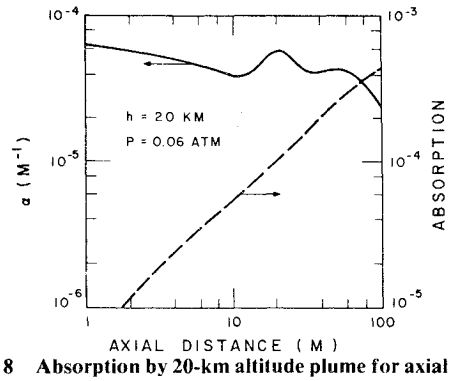

Fig. 8 Absorption by 20-km altitude plume for axial path.

around 12 km. We should point out, however, that this analysis on the possibility of condensation is valid for dry ambient air. Condensation may become possible over a wider range of altitudes if the ambient air also contains water vapor.

B. Plume at 20-km Altitude

Results of the three-dimensional code for a plume with the exit conditions given by the first line of Table 2 are shown in Fig. 7. The contours of constant H_2O concentration are found to follow the contours of constant temperature as expected. Since the self-broadening of H_2O is roughly five times larger than broadening due to collisions with air molecules, the absorption coefficient can be approximately calculated from the expression

$$\alpha(P_a,T,\psi_{H_2O}) = \alpha(P_a,T,\psi_{H_2O}=1)\psi_{H_2O}\left(\psi_{H_2O}+\frac{1-\psi_{H_2O}}{5}\right) \tag{31}$$

$\alpha(P_a,T,\psi_{H_2O}=1)$ is as given by Eq. (5). Equation (31) can then be used together with the results in Table 1 and Fig. 7 to evaluate the absorption coefficient to the $P(20)$ line of CO_2 along the axis of the plume where the absorption is the largest. The resulting absorption coefficient and the integrated absorption are plotted vs axial distance in Fig. 8. It shows that the integrated absorption at $x = 100$ m is negligible, being about 4×10^{-4}. Absorption integrated to $x\to\infty$ by analytical extrapolation is only about 8×10^{-4}, still negligible.

It is possible, however, that the actual absorption by water vapor may be much higher. The reason is that we have used the McClatchey tape to compute water-vapor absorption. Broadband measurements at 2000 K indicate absorption 100 times larger than that given by the McClatchey tape. Even with this possible factor of 100 taken into account, absorption by the plume at 20-km altitude is still small.

At an altitude above 20 km, there will be a barrel shock followed by a Mach disk. Inside the barrel shock the plume can be treated as expanding isentropically and the treatment of Sec. IV is valid. We found previously that absorption by water vapor was negligible, and this conclusion still holds here. Behind the Mach disk the plume has been shocked to ambient pressure and mixing with the surrounding air occurs. From the general considerations in Sec. V.A we do not expect any condensation in this portion of the plume. Since we found that at 20 km laser absorption by water vapor was negligible, and since at higher altitudes the plume will be larger and less dense, absorption by water vapor above 20-km altitude will be smaller than at 20-km altitude, i.e., also negligible.

C. Plume at Sea Level

Finite rate chemistry is not included in the plume entrainment computer code calculation at sea level because the chemistry is too fast and the axial step size required in order to follow accurately the chemistry would require excessively long computer times. Evaluation of the relevant reaction rates at sea level shows that the chemistry must be near equilibrium.

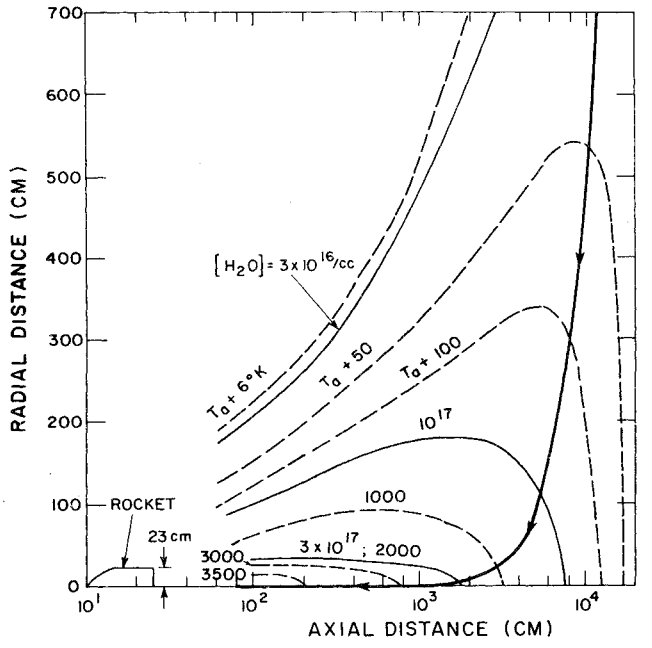

Fig. 9 Plume profile at sea level. The thick line corresponds to the laser beam trajectory with respect to the plume in a 10-m/sec cross wind.

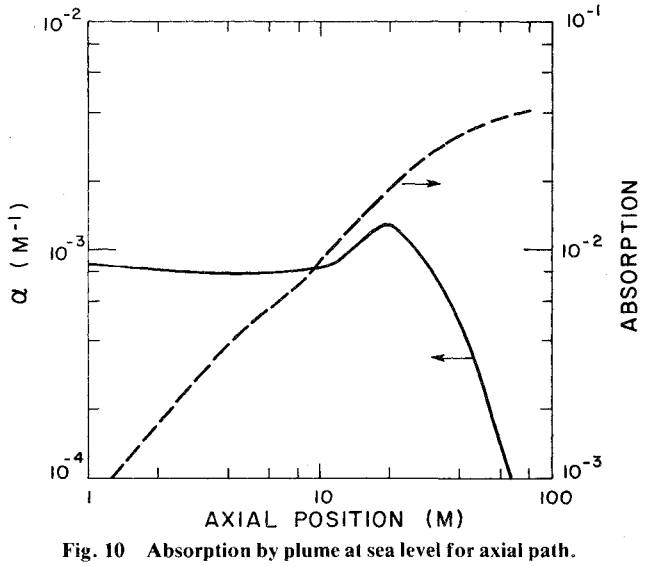

Fig. 10 Absorption by plume at sea level for axial path.

We have, therefore, assumed chemical equilibrium in our calculations.

The exit composition of the plume was as follows: $\psi_H = 0.25$, $\psi_{OH} = 0.15$, $\psi_{H_2} = 0.15$, $\psi_O = 0.12$, $\psi_{O_2} = 0.06$, and $\psi_{H_2O} = 0.23$. Other parameters can be found in the second line of Table 2. Figure 9 shows constant temperature and constant water-vapor concentration contours. Absorption by water vapor for an axial path length was calculated following the procedure outlined in the previous section and is shown in Fig. 10. The integrated absorption for an axial path length extending 100 m from the exit nozzle of the vehicle is found to be 4%. Longer path lengths do not lead to much larger absorption because of the rapid decrease in temperature.

Results based on water vapor absorption lines tabulated by McClatchey[9] indicate small absorption by the plume at sea level. On the other hand, the broadband measurements of Ludwig et al.[8] indicate that absorption could be as much as 100 times higher, leading to *catastrophic absorption* by the plume at sea level. High resolution measurements of H_2O absorption in the region of the CO_2 lines are needed before any firm conclusions can be drawn. If the laser beam is incident at an angle of 10 deg with the axis, the absorption can be reduced by a factor of 5 to 10, but the absorption, following the measurements of Ref. 8 would still be significant ($\sim 50\%$).

The possibility of a decrease in absorption caused by a cross wind has also been considered. It is estimated that a 10-m/sec cross wind will not appreciably bend the plume trajectory at distances less than 100 m. Since almost all of the absorption is caused by water vapor at $x < 60$ m, it is concluded that 10-m/sec cross winds have negligible effect on absorption by the plume.

VI. Summary and Conclusions

Condensation and absorption of CO_2 laser radiation in water-vapor plumes at various altitudes have been investigated with specific application to laser propulsion of rockets. Both absorption by water vapor and absorption/scattering by water droplets are considered. At high altitudes the plume behaves as an expansion into vacuum; the expansion leads to cooling and condensation. Absorption both by condensed water droplets and by water vapor was found to be negligible (5×10^{-3}). At intermediate and low altitudes (~ 20 km) the plume cools by entraining ambient air. We find that for typical engine conditions condensation is unlikely if the ambient air is dry, except possibly for a small altitude range near 12 km. Even if condensation were to occur, the concentration of water droplets would be too small to cause significant absorption. Absorption by water vapor was found to be negligible at 20 km ($< 10^{-3}$) and small at sea level ($\approx 4\%$). However, these results were obtained by using H_2O lines tabulated by McClatchey.[9] Measurements on the emissivity of H_2O flame products indicate[8] an absorption 100 times larger than those quoted earlier and point to the possibility of catastrophic absorption in sea-level plumes. The measurements of Ref. 8 are broadband, however, and high-resolution transmissivity measurements at the exact location of the CO_2 lines are urgently needed before definite conclusions may be drawn for the sea-level case.

References

[1] Kantrowitz, A. R., "Propulsion to Orbit by Ground-based Lasers," *Astronautics and Aeronautics*, Vol. 10, May 1972, pp. 74-76.

[2] Pirri, A. N. and Weiss, R. F., "Laser Propulsion," AIAA Paper 72-719, Boston, Mass., June 1972.

[3] Rom, F. E. and Putre, H. A., "Laser Propulsion," NASA TM-X-2510, April 1972.

[4] Legner, H. H. and Douglas-Hamilton, D., "CW Laser Propulsion," AIAA Paper 77-657, June 1977.

[5] Raizer, Y. P., "The Feasibility of an Optical Plasmatron and Its Power Requirements," *Soviet Physics JETP Letters*, Vol. 11, May 1970, pp. 302-305.

[6] Raizer, Y. P., "Heating of a Gas by a Powerful Laser Pulse," *Soviet Physics JETP Letters*, Vol. 21, Nov. 1965, pp. 1009-1017.

[7] Adiks, T. G., Aref'ev, V. N., and Dianov-Klokov, V. I., "Influence of Molecular Absorption on Propagation of CO_2 Laser Radiation in Terrestrial Atmosphere (Review)," *Soviet Journal of Quantum Electronics*, Vol. 5, May 1975, pp. 481-487.

[8] Ludwig, C., Ferriso, L., and Abeyta, C., "Spectral Emissivities and Integrated Intensities of the 6.3-μ Fundamental Band of H_2O," *Journal of Quantitative Spectroscopy and Radiative Transfer*, Vol. 5, Feb. 1965, pp. 281-290.

[9] McClatchey, R. A. and Selby, J. E., "AFCRL Atmospheric Absorption Line Parameters Compilation," Air Force Cambridge Research Laboratory, AFCRL-TR-73-0096, Jan. 1973.

[10] Goody, R. M., *Atmospheric Radiation, Vol. I, Theoretical Basis*, Oxford University Press, London, 1964, p. 115.

[11] Warga, J., "Minimizing Certain Convex Functions," *Journal of the Society of Industrial Applied Mathematics*, Vol. 11, Sept. 1963, pp. 588-593.

[12] *JANAF Thermochemical Tables*, 2nd ed., U.S. Dept. of Commerce, National Bureau of Standards, NSRDS-NBS 37, U.S. Government Printing Office, Washington, D.C., 1971.

[13] Svehla, R. A., "Thermodynamics and Transport Properties of the Hydrogen Oxygen System," NASA-SP3011, 1964.

[14] Kesselman, P. M. and Black, Y. I., "Thermo-Dynamical and Transport Properties of Water Steam at High Temperatures with account for Reality and Thermal Dissociation," *Transactions of the VII International Conference on the Properties of Water and Steam*, Paper D-11, Tokyo, 1968.

[15] Chapman, P. F., "Optimal Trajectories for Laser Powered Launch Vehicles," *AAS-AIAA Astrodynamic Specialist Conference*, Jackson, Wyo., Sept. 1977, to be presented.

[16] Ashkenas, H. and Sherman, F. S., "The Structure and Utilization of Supersonic Free Jets in Low Density Wind Tunnels," *Experimental Methods in Rarefied Gas Dynamics*, Vol. 2, edited by J. H. deLeeuw, Academic Press, New York, 1966, pp. 84-105.

[17] Albini, F., "Approximate Computation of Underexpanded Jet Structure," *AIAA Journal*, Vol. 3, 1965, pp. 1535-1537.

[18] Boynton, F., "Highly Underexpanded Jet Structure, Exact and Approximate Calculations," *AIAA Journal*, Vol. 5, 1967, pp. 1703-1704.

[19] Young, W. S., "Derivation of the Free-Jet Mach Disk Using the Entropy-Balance Principle," *Physics of Fluids*, Vol. 11, Nov. 1975, pp. 1421-1425.

[20] Feder, J., Russell, K., Lothe, J., and Pound, G. M., "Homogeneous Nucleation and Growth of Droplets in Vapors," *Advances in Physics*, Vol. 15, Jan. 1966, pp. 111-178.

[21] Shapiro, A. H., *The Dynamics and Thermo-Dynamics of Compressible Fluid Flow*, Vol. 1, Ronald Press Co., New York, 1953, pp. 73-87.